Atmos. Meas. Tech., 6, 751–763, 2013
www.atmos-meas-tech.net/6/751/2013/
doi:10.5194/amt-6-751-2013

Atmospheric Measurement Techniques
Open Access

A multi-year record of airborne CO_2 observations in the US Southern Great Plains

S. C. Biraud[1], M. S. Torn[1], J. R. Smith[2], C. Sweeney[3], W. J. Riley[1], and P. P. Tans[3]

[1]Lawrence Berkeley National Laboratory, Berkeley, California, USA
[2]Atmospheric Observing System Inc., Boulder, Colorado, USA
[3]NOAA Earth System Research Laboratory, Boulder, Colorado, USA

Correspondence to: S. C. Biraud (scbiraud@lbl.gov)

Received: 1 September 2012 – Published in Atmos. Meas. Tech. Discuss.: 25 September 2012
Revised: 4 March 2013 – Accepted: 5 March 2013 – Published: 15 March 2013

Abstract. We report on 10 yr of airborne measurements of atmospheric CO_2 mole fraction from continuous and flask systems, collected between 2002 and 2012 over the Atmospheric Radiation Measurement Program Climate Research Facility in the US Southern Great Plains (SGP). These observations were designed to quantify trends and variability in atmospheric mole fraction of CO_2 and other greenhouse gases with the precision and accuracy needed to evaluate ground-based and satellite-based column CO_2 estimates, test forward and inverse models, and help with the interpretation of ground-based CO_2 mole-fraction measurements. During flights, we measured CO_2 and meteorological data continuously and collected flasks for a rich suite of additional gases: CO_2, CO, CH_4, N_2O, $^{13}CO_2$, carbonyl sulfide (COS), and trace hydrocarbon species. These measurements were collected approximately twice per week by small aircraft (Cessna 172 initially, then Cessna 206) on a series of horizontal legs ranging in altitude from 460 m to 5500 m a.m.s.l. Since the beginning of the program, more than 400 continuous CO_2 vertical profiles have been collected (2007–2012), along with about 330 profiles from NOAA/ESRL 12-flask (2006–2012) and 284 from NOAA/ESRL 2-flask (2002–2006) packages for carbon cycle gases and isotopes. Averaged over the entire record, there were no systematic differences between the continuous and flask CO_2 observations when they were sampling the same air, i.e., over the one-minute flask-sampling time. Using multiple technologies (a flask sampler and two continuous analyzers), we documented a mean difference of < 0.2 ppm between instruments. However, flask data were not equivalent in all regards; horizontal variability in CO_2 mole fraction within the 5–10 min legs sometimes resulted in significant differences between flask and continuous measurement values for those legs, and the information contained in fine-scale variability about atmospheric transport was not captured by flask-based observations. The CO_2 mole fraction trend at 3000 m a.m.s.l. was 1.91 ppm yr^{-1} between 2008 and 2010, very close to the concurrent trend at Mauna Loa of 1.95 ppm yr^{-1}. The seasonal amplitude of CO_2 mole fraction in the free troposphere (FT) was half that in the planetary boundary layer (PBL) ($\sim$ 15 ppm vs. $\sim$ 30 ppm) and twice that at Mauna Loa (approximately 8 ppm). The CO_2 horizontal variability was up to 10 ppm in the PBL and less than 1 ppm at the top of the vertical profiles in the FT.

1 Introduction

The steady rise and seasonal cycle of atmospheric CO_2 mole fraction, first documented in detail at the Mauna Loa Observatory in Hawaii (Keeling, 1960; Pales and Keeling, 1965) and now at systematic monitoring sites around the world, has greatly contributed to our understanding of the carbon cycle and its relationship to a changing climate (Peters et al., 2010; Huntzinger et al., 2011). Nevertheless, uncertainties in the terrestrial carbon sink are among the greatest sources of uncertainty in predicting climate over the next century (NACP SIS, 2005; Friedlingstein et al., 2006; IPCC, 2007). In addition, for climate mitigation policy, there is a growing focus on testing and implementing methods for monitoring and verifying anthropogenic emissions (Mays et al., 2009; Shepson et al., 2011).

Atmospheric CO_2 mole-fraction observations, combined with inverse modelling, can be used to estimate land and ocean CO_2 sources and sinks at regional and continental scales (Tans et al., 1990; Enting et al., 1995; Rayner et al., 1999; Gurney et al., 2002; Ciais et al., 2010). In addition, airborne and tall tower observations of atmospheric CO_2 mole fraction are increasingly used to validate satellite-based or ground-based column CO_2 retrievals, test new airborne sensors (Abshire et al., 2010), and test the representativeness of ground-based observations (Xueref-Remy et al., 2011). Airborne campaigns with continuous CO_2 observations can also be used to investigate the horizontal and vertical variability of CO_2 mole fraction at multiple scales (Lin et al., 2004; Choi et al., 2008; Carouge et al., 2010).

However, there are many fewer airborne campaigns than there are land-based tower observations, few vertical profiles relating planetary boundary layer (PBL) and free troposphere (FT) mole fraction, few measurement programs with regular airborne observation missions, and poor uncertainty quantification (Hill et al., 2011). As a result, inversions are under-constrained (Ciais et al., 2010). Publications on modelling of atmospheric transport (Peters et al., 2007; Pickett-Heaps et al., 2011) and CO_2 surface flux inferred from atmospheric inversions (Stephens et al., 2007; Ciais et al., 2010) have called for more precise continental CO_2 mole-fraction vertical profiles. There are also errors in inversion estimates due to uncertainty in CO_2 observations themselves (Rayner et al., 2002), and regions poorly constrained by the measurements (Gurney et al., 2004). Measurement errors have been assumed to be small, based on laboratory calibration and analysis of known mole fraction in blind tests (Masarie et al., 2001). Another important source of error in inverse estimates is due to the very small mole-fraction differences that must be resolved among observing sites to infer spatial gradients in CO_2 surface fluxes. For example, Stephens et al. (2011) estimated that ≤ 0.2 ppm differences between two observatories located 500 km apart must be resolved for a resolution of $\sim 50\,\mathrm{g\,C\,m^{-2}\,yr^{-1}}$. For context, annual net ecosystem exchange measured at the Southern Great Plains (SGP) is typically around $-300\,\mathrm{g\,C\,m^{-2}\,yr^{-1}}$; Riley et al. (2009). Likewise, Marquis and Tans (2008) set a goal of ≤ 0.1 ppm comparability for measurements used in global atmospheric monitoring. Inter-laboratory differences assessed from round-robin comparison have shown that the uncertainty in measured CO_2 from several laboratories is approaching 0.1 ppm (WMO, 2011), and such comparability is becoming mainstream, thanks to the standardization of observational procedures and commercialization of new plug-and-play ground-based instruments developed by companies like LI-COr, Los Gatos Inc., Picarro Inc., and others. Nevertheless, the goal of ≤ 0.1 ppm has eluded aircraft-based observations, because of the difficulty in ensuring high-accuracy measurements under changing ambient pressure and temperature in a mechanically stressed environment.

We designed our airborne program to provide a well documented data set able to meet the science needs identified above. Our high frequency vertical profiles from SGP have proven useful in validating atmospheric CO_2 column measurements from ground-based Fourier transform spectrometers (Wunch et al., 2010, 2011) and satellite-based retrievals (Kulawik et al., 2010, 2012; Kuai et al., 2013). The objectives of this paper are to: (1) use multiple technologies to validate airborne observations collected in the US Department of Energy (DOE) Atmospheric Radiation Measurement (ARM) Climate Research Facility (ACRF) SGP; (2) present results from a multi-year record of CO_2 observations to explore seasonal, vertical, and high frequency patterns in continuous CO_2 observations; and (3) provide documentation and uncertainty quantification to enable application of these observations to a broad set of research questions.

2 Methods

The ARM program supports a large testbed ($\sim 300 \times 300$ km) for measurements and modelling in the US Southern Great Plains (Ackerman et al., 2004). All atmospheric and climatic variables measured in the ACRF are available from the ARM Data Archives (www.arm.gov). The heart of the SGP site is the heavily instrumented central facility (CF) located at 36°37′ N, 97°30′ W, 314 m a.m.s.l., near the town of Lamont, Oklahoma. Forests dominate the eastern one-third of Oklahoma and the ACRF; the western half of the state is primarily agricultural and grassland. Spring and early summer is generally characterized by active weather patterns, with numerous frontal systems and precipitation. In contrast, fall is usually dry and sunny.

The Lawrence Berkeley National Laboratory (LBNL) ARM Carbon Project started in 2001 with state-of-the-art CO_2 atmospheric mole-fraction measurements (Bakwin et al., 1998) from a 60 m tower located at the CF, and a system of fixed and mobile instruments for measuring CO_2, water, and energy fluxes, deployed at selected locations around the SGP region (Billesbach et al., 2004; Fischer et al., 2012). In 2002, airborne observations over the central facility started as part of a joint effort between the ARM program, the Earth System Research Laboratory (ESRL) of the US National Oceanic and Atmospheric Administration (NOAA), and the LBNL ARM Carbon project. The focus of this project is to collect aerosol and trace-gas vertical profiles on board a small manned aircraft (Cessna 172). The typical flight pattern consisted of a series of 12 level legs at standard altitudes, ranging from 460 m to 5500 m a.m.s.l. centered over the 60 m CF tower (Fig. 1). Each leg was flown at constant altitude and lasted 5 (below 1800 m) or 10 (above 1800 m) minutes. Because of additional DOE restrictions on instrument flight rules, these flights had a strong daytime, clear-sky bias (Fig. 2). In contrast to short-duration airborne observations presented in previous studies (Langenfelds et al.,

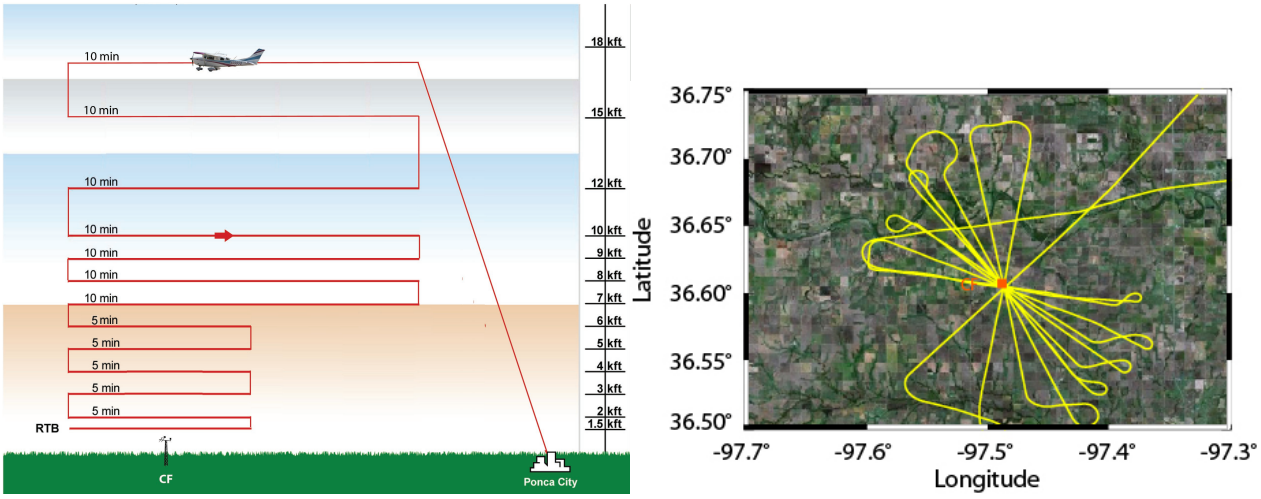

Fig. 1. (Left) Vertical flight pattern for flights deployed over the ARM/SGP from 460 m to 5500 m a.m.s.l. (Right) Horizontal projection of flight pattern centered on the tower of ARM/SGP, overlayed over a true color land cover picture of the region. Red square shows the location of the SGP central facility 60 m tower. Orientation of the flight pattern depends on prevailing winds and changes with altitude to avoid contamination by platform exhaust. Yellow lines show the flight path for a typical flight (24 October 2011).

2003; Font al., 2008; Chen et al., 2010; Haszpra et al., 2012; Karion et al., 2013), our observations were the first routine atmospheric CO_2 profiles co-located with simultaneous continuous ground CO_2 flux and mole-fraction measurements in the US and/or continental sites. Further, they were for a time the only such measurements conducted routinely over the agricultural heartland of North America. Flask samples are analyzed by NOAA ESRL for a suite of carbon cycle gases and isotopes, thereby linking all flights to the global cooperative air-sampling network (http://www.esrl.noaa.gov/gmd/ccgg/flask.html). In 2006, the aircraft was upgraded to accommodate a larger payload (Cessna 206), and instrumentation for flask collection at 12 heights was added. In 2007, continuous CO_2 mole-fraction measurements were initiated, making these the only routine, long-term, continuous CO_2 profile observations over the US. In 2008, the airborne program expanded its scope and became a separate project: the ARM Airborne Carbon MEasurements Project (ACME). Data collected under this program can be accessed through the ARM web-based portal (http://www.arm.gov/campaigns/aaf2008acme). All CO_2 observations in this paper are reported in the WMO/GAW X2007 scale.

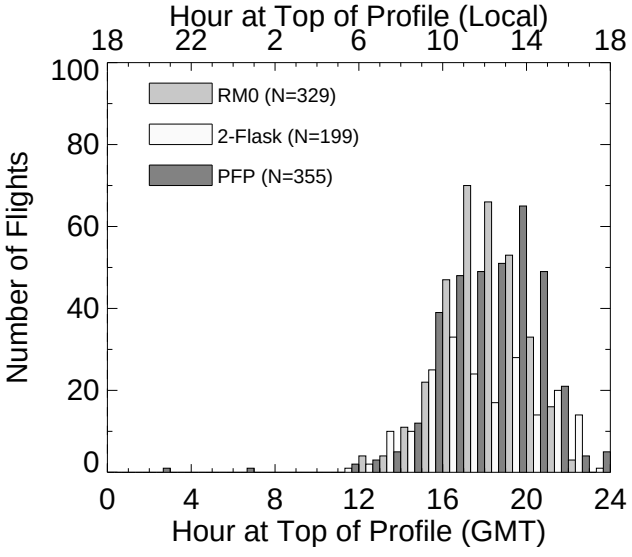

Fig. 2. Frequency histogram of hour at which highest altitude sampling took place, sorted by sampling system.

2.1 Flask-based observation methods

Starting in 2002, we collected bi-weekly flasks as part of the NOAA/ESRL Global Monitoring Division Aircraft Group. Flask samples were, and continue to be, analyzed in Boulder by the Carbon Cycle Greenhouse Gases group (CCGG) for CO_2, CH_4, CO, H_2, N_2O, and SF_6; and by the Institute of Arctic and Alpine Research (INSTAAR) for many volatile organic compounds (VOCs) such as acetylene (C_2H_2) and propane (C_3H_8). A pair of flasks (2 L each) was collected at a given altitude per flight, either in the mid-PBL ($\sim$ 600 m), or in the FT ($\sim$ 3000 m). If the pair of flasks was collected in the mid-PBL, we tried to coordinate airborne sampling with ground flask sampling, yielding near-synchronous collection of samples at 60 m and 600 m. A total of 676 flasks were collected and analyzed between September 2002 and January 2006 with this system, leading to 334 pairs of observations. Among those pairs of flasks, 199 were collected in the FT and 135 were collected within the PBL (including 51 ground coordinated samplings).

The two-flask sampler was upgraded in 2006 and a 12-flask sampler, designed by NOAA/ESRL, was installed on the aircraft and has been used up to the present. With this technology, samples are collected on each horizontal leg of the vertical profile described in the section above. The flask sampler has two components: (1) a rack-mounted precision compressor package (PCP) and (2) a portable multi-flask package (PFP). Prior to each flight, the pilot connects a new PFP to the resident PCP. An automatic test is then performed to check for leaks and plumbing problems. The PCP is connected to a platform display that allows the pilot to trigger sampling when the desired location and altitude have been reached. For each sample, the inlet is first flushed with 5 L of ambient air; then the flask itself is flushed with 10 L of ambient air. After the inlet is flushed and the flask is complete, the downstream valve of the flask is closed to achieve a 40 psia pressurization of the flask. After each flight, the filled PFP is returned to the NOAA laboratory for analysis of the suite of trace gases. As of July 2012, a total of 3868 flasks had been collected, constituting 332 vertical profiles. Due to infrastructure requirements for maintaining a large stock of operational PFPs and conducting the intensive analyses performed on the flask samples, we are currently collecting flask samples on only one out of every three-four flights.

2.2 Continuous CO_2 observation methods

In June 2007, a continuous NDIR CO_2 analyzer (hereafter referred to as RM0 for rack mount system #0), built by Atmospheric Observing System Inc. (AOS, Boulder, Colorado), was deployed on the aircraft (Fig. 3) and has been used ever since. This type of analyzer has been used by other research groups located in Spain, Germany, and Hungary (Font et al., 2008; Chen et al., 2010; Haszpra et al., 2012). The core of the system is a nickel-plated, differential aluminum analyzer and gas processor, designed around two identical nickel-plated gas cells, one for reference gas and the other for sample gas. Radiation sources are collimated through the gas cells, and then concentrated onto temperature-controlled photodetectors. Absorption of the radiation serves as the measure of CO_2 mole fraction. There are no moving parts, and the sources are modulated electronically at 8 Hz. A pair of identical radiation filters, one in front of and the other behind, each gas cell isolates radiation to the targeted molecular band centered at 4.26 µm with a width of 0.20 µm. The final piece of the analyzer is the custom digital demodulator, which converts the differential AC signal generated by the analyzer into a DC response. The resulting DC signal is an averaged count of CO_2 mole fraction over a specified bandwidth (currently 8 Hz) reported in volts, and a corresponding sample dew point temperature (DPT). The system controls flow rate, pressure, and valve switching. The remainder of the system consists of compressors, dry reference gases (called responsivity, zero, and target in the text below), an air drier (a combination of a semi-permeable membrane (Nafion) followed by a cartridge of magnesium perchlorate (MP)), and electrical cables.

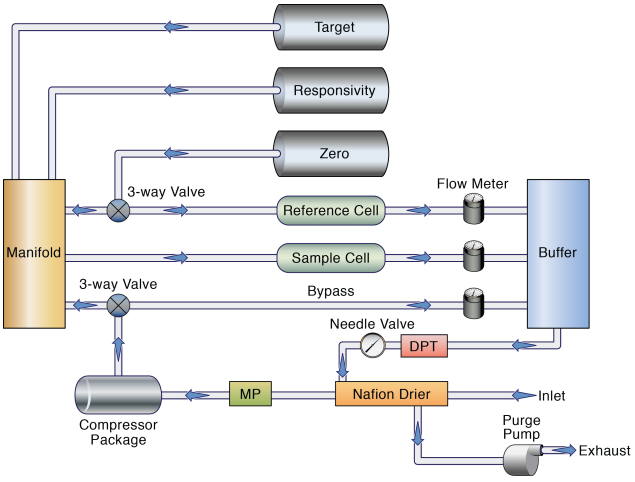

Fig. 3. Air flow for RM0 continuous analyzer. Note that there are feedbacks loops between proportional valves (not shown) and the three flow meters and pressure transducer of the buffer volume. MP is the chemical drier filled with Magnesium Perchlorate. DPT is the dew point temperature sensor.

Forty-five minutes before take-off, the pilot turns the system on by flipping a single power switch and operating three mechanical valves that enable air flow between the subsystems and isolating the plumbing from outside air when it is not being used. The analyzer operates autonomously during flight. The steps are reversed at the end of a mission. Data are typically downloaded within minutes after each flight. Diagnostics of the system (lags, flow rates, drying efficiency, temporal variability) and decomposition into vertical profiles and transects are done in final form in about 10 min by a program developed and written by AOS, Inc. Additional software is used to track reference gas usage and diagnose the pneumatic and electronic performance of the analyzer. The system is intended to be used to measure CO_2 in the atmosphere (350 ppm to 450 ppm range). It has negligible sensitivity to the motion of the platform. Typically, the air stream reaching the sample cell has a dew point of $-55\,^{\circ}C$, corresponding to less than 100 ppm water vapour.

During the warm-up cycle, the reference cell is flushed with differential zero gas (which is the only gas that the cell ever sees) for two minutes at 0.2 slpm to make sure the reference cell is dry ($-55\,^{\circ}C$ dew point temperature) and fully flushed. After the first two minutes, the flow in the reference cell is alternatively turned down to no flow (for 20 s) or to a trickle flow (0.01 slpm for 3 min). During that time, the sample cell is flushed at 0.2 slpm with differential zero gas (for 20 s) or dried ambient air (for 3 min). This cycle is repeated 6 times. The warm-up phase ends with constant flushing of the sample cell using dried atmospheric ambient air for 11 min. The warm-up cycle, which consists of flushing

the plumbing and both cells, takes about 45 min and must be completed prior to take-off. After the initial 45 min, the measurement cycle starts, consisting of calibration gas measurements (20 s), followed by 3 min sampling measurements. The calibration is a differential zero, a target, or a responsivity gas. Every fifth differential zero is alternatively replaced by either a responsivity or a target gas measurement (Fig. 4).

Regular maintenance consists of: (1) replacing the magnesium perchlorate cartridge every 45 flight hours (about every 15 flights for our project) to minimize the effects of water vapour; (2) recharging the reference gases every 240 flight hours (about every 80 flights for our project); and (3) verifying the calibration of the reference gases using 14 field-standard cylinders ranging from 350 to 450 ppm (WMO X2007 scale). As of March 2012, the original analyzer (RM0) has performed with an accuracy of < 0.2 ppm at 1 Hz (including bias) for more than 329 missions (~ 1000 flight hours). The calibration of the on-board cylinders (differential zero, responsivity, and target) is crucial and done when cylinders are installed in the analyzer system on the platform, i.e., in the field, replicating measurement conditions. To achieve this, field calibration cylinders are connected to a buffer volume (100 mL), vented to ambient pressure. Calibrating the machine at the inlet of the system (not only the analyzer) is important to account for all biases associated with the machine (drier, plumbing, analyzer itself). It is worth noting that we run reference gases through the drier when we perform calibrations of the on-board cylinders on the ground, but not in flight.

2.3 Supporting data

Between 2002 and 2008, relative humidity (RH) and temperature (T) vertical profiles were recorded continuously as part of the ARM in situ aerosol profiles (IAP) campaign. Since 2008, RH and T profiles have been collected as part of the on-board ozone analyzer. Because these ancillary data are collected by independent data acquisition systems, we do not always have a full set of observations of RH, T, and continuous CO_2.

2.4 Repeatability and accuracy

Immediately after collection, each flask package is returned to NOAA/ESRL for analysis of as many as 55 trace gases. A non-dispersive infrared analyzer measures 100 mL of sample for CO_2 with a repeatability of ± 0.03 ppm (Conway et al., 1994). The repeatability of the instrument is determined from 1 standard deviation of ~ 20 aliquots of natural air measured from a known cylinder. Note that flask-based observations have a documented bias of ~ 0.007 ppm per day of storage (http://www.esrl.noaa.gov/gmd/ccgg/aircraft/qc.html) due to differential diffusion of CO_2 through the Teflon O-ring seals located at the end of each flask. This bias is not taken into account when flask-based measurements are reported.

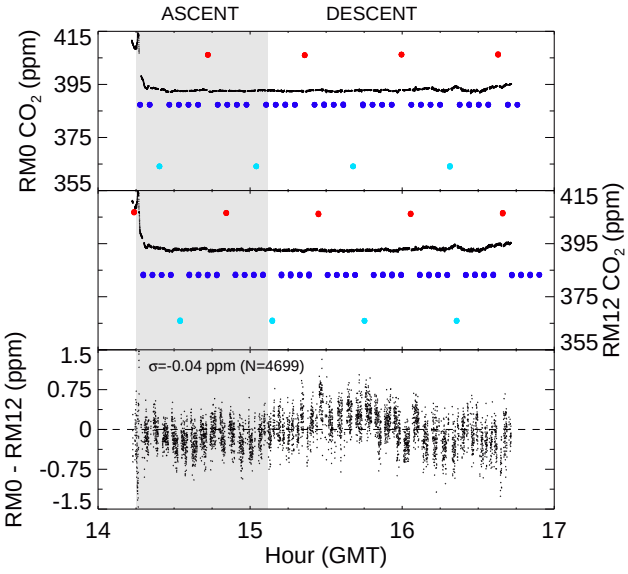

Fig. 4. CO_2 mole fraction collected on 21 March 2011 by the two continuous analyzers. Top and middle panels show observations by RM0 and RM12, respectively, organized by ascent and descent. Red circles give target, dark blue circles give zero, light-blue circles give responsivity, and black dots give unknown sample measurements (1 Hz). The bottom panel shows the mean difference (-0.04 ppm) between CO_2 mole fraction measured using the two continuous systems.

Considering that it takes on average about 3 weeks for a flask to be shipped to the sampling location, collected, and returned to the lab for analysis, there may be a storage offset of as much as -0.2 ppm.

On 16 March 2011 a second analyzer built by AOS (RM12), was deployed on the aircraft with an intentional 15 seconds plumbing delay relative to RM0. Except for having an older, noisier generation of electronics, RM12 is very similar in operation to RM0. The two AOS analyzers (RM0, RM12) ran independently, operated with separate calibrations, had their own compressors, and pulled air from an inlet also servicing the flask package. This intentional delay makes it possible to observe solitary transient phenomena and bias against any platform-induced effects that should have zero delay. To assess the performance of both systems on the ground, a common gas source (a cylinder on board the aircraft) of known mole fraction was measured by both continuous analyzers for one hour on 2 August 2011 (Fig. 5). Repeatability for RM0 and RM12 was 0.10 ppm (standard deviation of $N = 2814$ observations) and 0.25 ppm (standard deviation of $N = 2937$ observations), respectively. Accuracy, including the specific mission calibration and accuracy of reference-gas delivery, was 0.13 ppm and -0.06 ppm for RM0 and RM12, respectively.

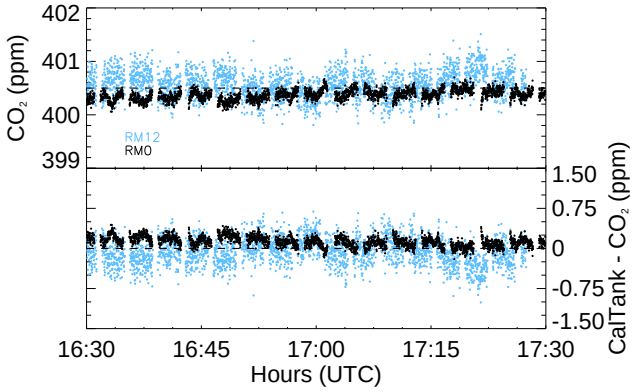

Fig. 5. Accuracy and repeatability in the aircraft on the ground for the two continuous CO_2 systems (black = RM0 and blue = RM12) estimated from the measurement of CO_2 mole fraction delivered by a cylinder maintained at ambient pressure and flushed continuously by a stream of reference gas calibrated earlier in the laboratory. Repeatability for RM0 and RM12 as shown on top panel was 0.10 ppm (standard deviation of $N = 2814$ observations) and 0.25 ppm (standard deviation of $N = 2937$ observations), respectively. Accuracy as shown on bottom panel, including the specific mission calibration and accuracy of delivery of reference gas, was 0.13 ppm and −0.06 ppm for RM0 and RM12, respectively.

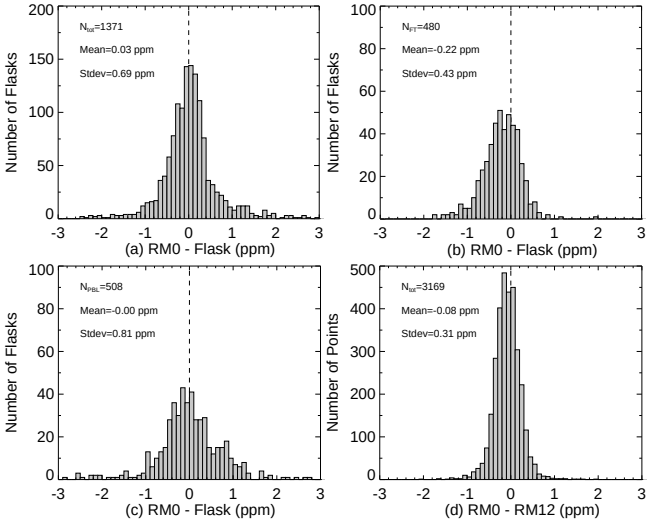

Fig. 6. Distribution of the difference calculated between: **(a)** all continuous (RM0) and flask measurements, **(b)** RM0 and flask measurements collected above 3500 m, i.e. in the FT, **(c)** RM0 and flask measurements collected below 1000 m, i.e. within the PBL, during the November 2007 through March 2012 time period. The distribution of the difference calculated between two continuous CO_2 analyzers (RM0 and RM12) from observations collected between March 2011 and August 2011 is shown in panel **(d)**. Each point refers to the mean difference between a flask sample and the 1-min average of the continuous observations centered around the time that the flask was filling, one for each of the 12 steps during descent.

2.5 Data quality check

To improve confidence in the flask observations, in 2002 we started collecting a pair of flask samples either in the FT, or in the mid-PBL. Besides the usual assessment of flask conditioning and actual measurement quality control, which includes the difference between the two members of the pair (the pair was flagged if the pair difference is larger than 0.5 ppm), we also cross-referenced sampling date and time, latitude, longitude, and elevation for each individual flask. Around 5 % of the flask measurement metadata initially reported were inconsistent with actual observation metadata and were subsequently corrected.

In 2006, we began observations with the 12-flask system. Between June 2007 and March 2012, consistency checks of our airborne observations were performed by comparing continuous measurements and flask-based observations. This process was a cross-validation between two independent systems (rather than merely a validation of one system by the other) and permitted detection of possible issues with either system. During this period, 359 RM0-based vertical profiles and 2144 flask samples were collected. Figure 6a shows the distribution of the difference between 1-min averaged RM0 data and the corresponding flask data. Across this dataset, there is no significant offset between the two systems (mean difference of −0.08 ppm, Fig. 6a), and the standard deviation of the difference is 0.6 ppm. The distribution of the difference has a fairly long tail, meaning that sometimes the flask-based and RM0 observations do not compare well with each other. The timing of sample acquisition of a fluctuating atmosphere by the flask technology is probably a significant source of noise for this comparison (Fig. 6b and c). The "flushing + acquisition" window of the flasks is tens of seconds, and fluctuations in the PBL can be large (a ppm or more) during that time interval for an aircraft flying at approximately 100 m s^{-1} (see discussion below on observed horizontal variability). Figure 6b and c show that the standard deviation of the mean difference between RM0 and flask samples is smaller in the FT (0.47 ppm) than in the PBL (0.67 ppm).

As mentioned above, on 16 March 2011 RM12 was deployed on the ACME platform. RM12 showed a repeatability of 0.25 ppm (standard deviation of $N = 2937$ observations), due to the use of noisier earlier generation electronics. Figure 7 gives an example of observations collected using all three systems (RM0, RM12, and PFP) during an 28 April 2011 flight. The mean and standard deviation of the difference between RM0 and RM12 was 0.06 ppm and 0.3 ppm, respectively. Noise in the difference between observations from the pair of analyzers should equal the square root of the sum of the square of the accuracy of each analyzer. For thirty-seven flights between 16 March 2011 and 30 July 2011, comparisons made in the same manner gave a mean RM0–RM12 difference of −0.08 ppm and a standard deviation of the difference of 0.31 ppm. The standard

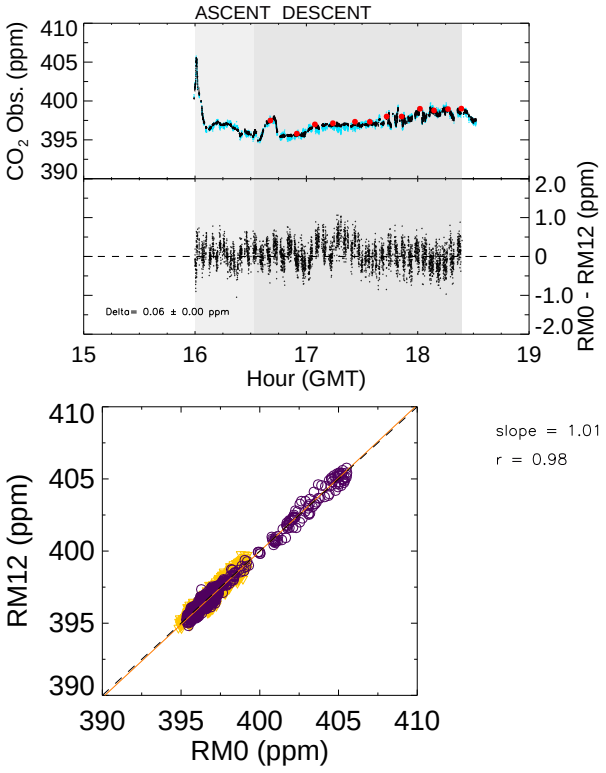

Fig. 7. CO_2 mole fraction collected using multiple technolgies (RM0, RM12, and PFP) during an 28 April 2011 flight. The top panel shows the time series of CO_2 mole fraction measured using all three systems. The middle panel shows the mean difference (0.06 ppm) between CO_2 mole fraction measured using the two rack mount systems. The standard deviation of the difference is 0.3 ppm. The bottom panel shows a regression of the observations made using RM0 and RM12 systems. Open purple and yellow circles correspond to the ascent and descent parts of the flight, respectively.

deviation of the difference was largely controlled by the electro-optical noise of RM12 (Fig. 6d).

The use of multiple technologies on the ACME platform is important, because of the substantial changes in ambient humidity, pressure, and temperature that the platform experiences during a flight. Mean absolute mole fraction measured by a continuous analyzer are validated by comparison with flask observations. An additional level of validation is made by comparing continuous observations with each other, one analyzer having an intentional lag of 15 s with respect to the other one. Atmospheric fluctuations must be detected by both analyzers, one analyzer's response to these fluctuations lagging behind the other analyzer's response by 15 s. Any fluctuations happening simultaneously or with some other differential lags in both analyzers must be viewed as artifacts. This approach has improved objectivity of the airborne platform substantially by allowing detection and diagnostics of problems in all parts of the system: leaks in the flask sampler compressor package, drift in calibration cylinders used by the continuous analyzers, and aging of the inlet tubing.

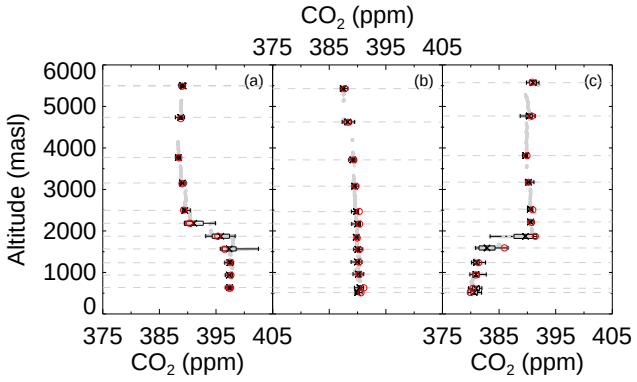

Fig. 8. Vertical profiles of CO_2 in wintertime (**a**; 18 March 2009), well-mixed condition (**b**; 20 May 2009), and summer/fall (**c**; 27 October 2010). Gray dots shows continuous observations collected by the RM0 system. CO_2 mole fraction collected during horizontal legs of the flight have been binned to calculate simple statistics: minimum and maximum (black vertical segments), mean (black cross), and standard deviation (rectangle) of CO_2 mole fraction. Open red circles show CO_2 mole fraction measured from flasks.

3 Results and discussion

3.1 Typical atmospheric CO_2 profiles

Observed mole-fraction patterns are driven by CO_2 sources and sinks, as well as atmospheric transport (Gerbig et al., 2003; Choi et al., 2008). Flights were usually made in the afternoon (Fig. 2), when the PBL is fully developed. Vertical mixing in the PBL responds to land-surface properties such as temperature, moisture, and wind speed (Denning et al., 1995). Above the PBL, the atmosphere is usually non-turbulent and stratified, and CO_2 mole fraction are influenced by large-scale circulation (Stull, 1988). Figure 8 shows vertical CO_2 mole-fraction profiles collected during the descent portion of three typical flights (Fig. 8a: 18 March 2009; Fig. 8b: 20 May 2009; and Fig. 8c: 27 October 2010), using the RM0 analyzer and flask-based measurements. The observed variability across any particular horizontal leg demonstrates the difficulty of comparing CO_2 flask and continuous measurements. The differences between flask and RM0 observations are larger within the PBL and where large horizontal variability is observed by RM0. In addition, flask-based observations do not give information about fine-scale variability in CO_2 mole fraction.

During wintertime in general and for the flight described in Fig. 8a specifically, plant respiratory flux and anthropogenic emissions dominate the land–atmosphere exchanges (Pataki et al., 2007). Figure 8a shows that the CO_2 mole fraction in the PBL are relatively uniform around 397 ppm, while the CO_2 mole fraction above the PBL are 10 ppm lower. During summer and fall, in general and for the flight described in Fig. 8c, vegetation photosynthesis drives the land–atmosphere exchange (Bakwin et al., 1998). In those seasons,

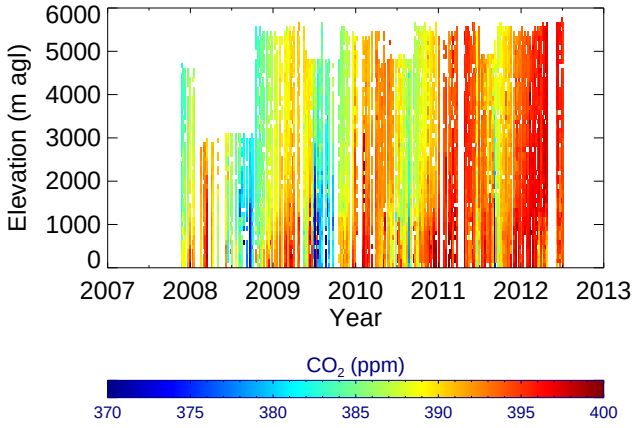

Fig. 9. Time series of continuous CO_2 vertical profiles collected from November 2007 through 31 July 2012 from RM0.

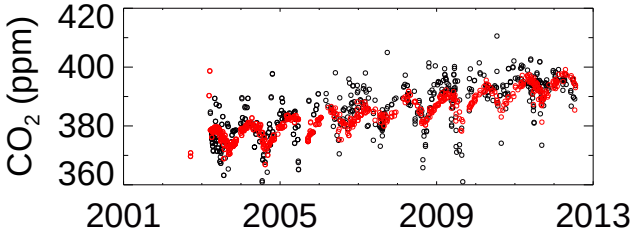

Fig. 10. Time series of CO_2 vertical profiles collected from September 2002 through July 2012 from flasks collected at 3000 m (above the PBL, red circles, $N = 740$) and 1000 m (below the PBL, black circles, $N = 604$).

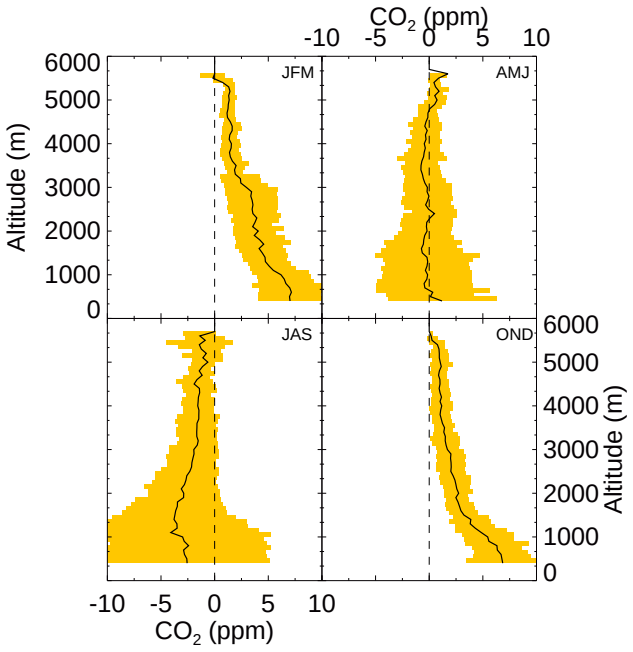

Fig. 11. Climatology of all vertical profiles collected between 2007 and 2010, shown as an anomaly relative to mole fraction at Mauna Loa (Mauna Loa data not yet available in 2011). CO_2 observations at the Mauna Loa observatory have been interpolated on a weekly basis to normalize flight profiles. CO_2 observations are binned into 100 m altitude pixel and weekly flight profiles. Each quadrant of the graph corresponds to a 3-month average climatological vertical profile (JFM: January-February-March, ...). The solid black line shows the mean vertical profile calculated across each 3-month average, and the yellow shaded area shows one standard deviation around the average value.

the vertical pattern is reversed; CO_2 mole fraction in the PBL are relatively uniform around 381 ppm, while CO_2 mole fraction above the PBL are 10 ppm higher. Figure 8b shows relatively uniform CO_2 mole fraction from the top to the bottom of the vertical profile. May is a transition time in Northern America, with the land-surface dominance shifting from a plant respiration to a plant uptake, even if May is the month of peak uptake by regionally grown winter wheat (Riley et al., 2009), resulting in similar mole fraction above and below the PBL. Summer, fall, and winter conditions are associated with a large difference in CO_2 mole fraction across the top of the PBL ($\sim$ 2000 m). Although this fairly large gradient across the PBL was observed using continuous measurements of CO_2 from a tall tower (Helliker et al., 2004) or flasks collected from an aircraft (Williams et al., 2011) has been used to estimate net CO_2 flux, uncertainty on those estimates has not been well quantified, and the use of regular continuous airborne observations could help improve estimates of flux.

3.2 Seasonal patterns

Ground-based observations in the SGP show CO_2 mole fraction varying diurnally by up to 100 ppm and seasonally by $\sim$ 15 ppm, due to ecosystem exchanges with the atmosphere, proximity to fossil sources, changes in PBL depth, and exchanges with the FT (Pearman et al., 1983; Enting and Mansbridge, 1991; Denning et al., 1995). CO_2 seasonal cycle amplitude and trend can be estimated at different elevations using both continuous and flask observations. Figure 9 shows continuous CO_2 observations collected using RM0 between November 2007 and July 2012. Figure 10 shows CO_2 observations collected from flasks between September 2002 and July 2012. The seasonal maximum and minimum CO_2 mole fraction occur in March and August of each year, respectively, reflecting photosynthetic drawdown and terrestrial ecosystem respiration (Conway et al., 1994). The timing of the seasonal cycle is nearly the same at both heights. Over the 10 yr record, the peak-to-peak amplitude of the seasonal cycle is $\sim$ 15 ppm at 3000 m (FT), and $\sim$ 30 ppm at 1000 m (PBL) (Figs. 9 and 10). The difference in the seasonal cycle amplitude between the two heights is large ($\sim$ 15 ppm) because the seasonal amplitude of CO_2 in the PBL is amplified by the rectifier effect of seasonal variation in PBL height covarying with CO_2 sources and sinks (Denning et al., 1995).

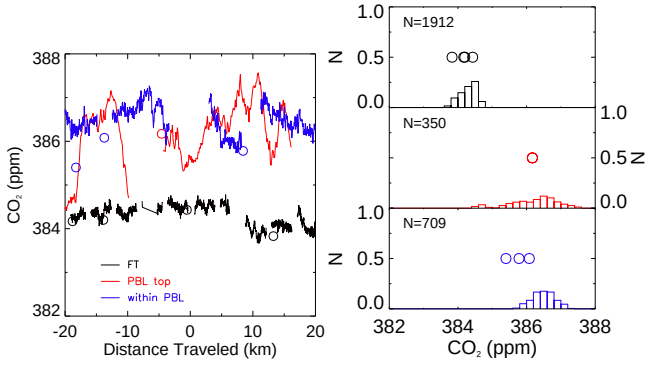

Fig. 12. (Left panel) Observed CO_2 mole fraction from flasks (circles) and RM0 across horizontal legs in the FT (black), at the PBL top (red), and within the PBL (blue), for the 4 August 2008 flight. The FT line includes observations from three horizontal legs between 2500 m and 3200 m a.m.s.l.; the PBL top line includes observations from one horizontal leg at ∼ 1000 m a.m.s.l.; and the within PBL line includes observations from two horizontal legs between 500 m and 600 m a.m.s.l. The PBL legs were 5 min and are scaled to fit the same distance axis. (Right panel) The same data as in the left panel, plotted as probability distribution functions for FT, PBL top, and within PBL CO_2 mole fraction. Data were non-normally distributed in the FT and at the PBL top; these types of non-normal distributions were common throughout the five years in all three altitude regimes. There was an offset, or bias, between the flask values and the mean value of the continuous data in the PBL but not in the FT.

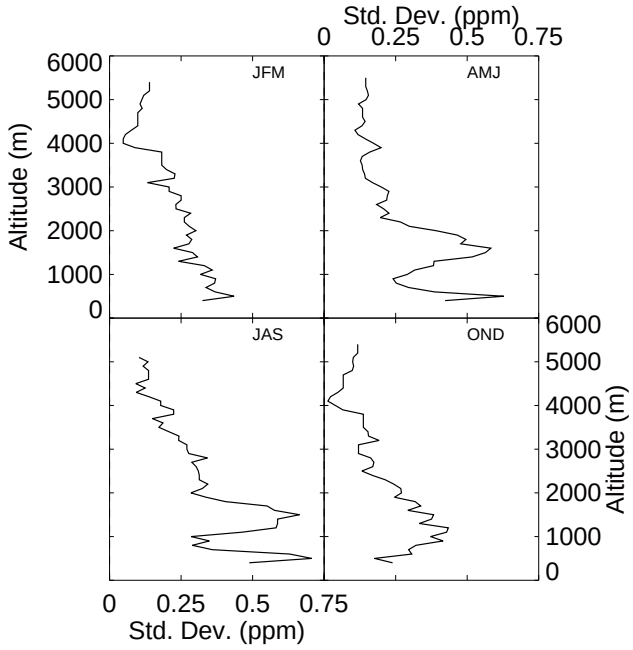

Fig. 13. The standard deviation of the differences in CO_2 mole fraction between RM0 and flasks collected between 2007 and 2012. The RM0 data were binned to 1-min averages. Each quadrant of the graph corresponds to a 3-month average climatological vertical profile.

Other work has shown that covariance of atmospheric transport also contributes to the large seasonal amplitude observed in the SGP (Williams et al., 2011). The CO_2 mole-fraction trend at 3000 m estimated from RM0 observations is ~ 1.91 ppm yr^{-1} between 2008 and 2012, very close to the Mauna Loa trend of 1.95 ppm yr^{-1} over the same period.

Although historical time series of vertical profiles give valuable information (Figs. 9 and 10), atmospheric transport modelers are usually more interested in weekly or monthly average observations rather than a particular observation or flight. A seasonal composite of vertical CO_2 mole-fraction profiles between 2007 and 2011 (Fig. 11) demonstrates the regional effects of plant activity and anthropogenic sources relative to the well-mixed northern hemispheric signal recorded at Mauna Loa. The CO_2 vertical gradient between the FT and PBL is negative (~ -7 ppm) in winter and positive (~ 4 ppm) in summer. No vertical gradient was observed when all flights were averaged over spring. It is important to remember that Fig. 11 shows a composite of flights, meaning that individual flights occasionally had very different vertical structures, as indicated by the relatively large measured standard deviation. The standard deviation is larger in the PBL than in the FT, decreasing monotonically with altitude, reflecting hemispheric mixing. It remains significant (> 1 ppm) relative to the instrumental precision of 0.1 ppm, up to 5000 m a.m.s.l.

3.3 Horizontal variability with altitude

As described earlier, large variability in the CO_2 mole fraction across individual horizontal legs was commonly observed, with three implications for carbon cycle studies (Fig. 8).

First, the horizontal variability sometimes resulted in biases between flask and continuous CO_2 measurements when the flask values were compared to continuous data for the whole flight leg. In that situation, the use of instantaneous flask measurements to characterize CO_2 mole-fraction gradients to inform atmospheric inversions of surface CO_2 exchanges may also be biased. We present several examples of CO_2 mole-fraction heterogeneity and mean biases across seasons. To illustrate vertical and horizontal CO_2 mole-fraction variability, we chose a single flight from 4 August 2008, a day that is typical of this time of year in the SGP, i.e., after the dominant crop (winter wheat) has senesced, the pasture is at peak productivity, and the PBL is relatively high (Fig. 12). On this afternoon, FT continuous and flask CO_2 mole fraction were 384.3 ppm (stdev = 0.24 ppm) and 384.2 ppm, respectively. The continuous CO_2 mole fraction had a left-skewed probability distribution, and there was no significant difference between continuous and flask measurements. Within the PBL, continuous and flask CO_2 mole-fraction means were 386.5 (stdev = 0.32 ppm with a roughly symmetric probability distribution) and 385.8 ppm,

respectively. The bias between the means of the continuous and flask CO_2 mole-fraction measurements was 0.7 ppm. The CO_2 mole fraction at the PBL top were much more variable (386.2 ppm; stdev = 0.69 ppm) with a flatter and bimodal probability distribution, and the single flask value was 0.41 ppm lower than the mean of continuous data. Figure 13 characterizes the variability between flask and continuous data over the five years of observations by elevation. In general: (1) horizontal variability and consequent differences between continuous and flask CO_2 mole-fraction measurements were larger in the PBL than in the FT, and summer than in winter; (2) maximum variability was seen at the top of the PBL, except in spring, when it was maximum near the surface. We note that the horizontal leg segments of the vertical profiles are 5 and 10 min long (length $\sim$ 20 km and $\sim$ 40 km), above and below 2000 m, respectively, which might not capture the full extent of the regional horizontal variability.

Second, the horizontal variability had vertical and seasonal structure, with more variability at the PBL-FT interface than above or below, and more variability when there was a larger mole-fraction gradient between PBL and FT to mix across that interface. The large heterogeneity in CO_2 mole fraction near the PBL-FT interface may indicate discontinuous and sporadic exchanges across this interface and may be relevant to studies of cloud convection, subsidence and entrainment, and inversion-based inferences of surface CO_2 exchanges. Although the single-flask mole-fraction values were usually within 0.2 ppm of the associated altitude-mean from continuous observations, the large horizontal variability indicates that transport processes may not be well represented by the use of flask observations alone. The atmospheric inversion models cited above have applied weekly–monthly averages of mole-fraction measurements, and very often these measurements are taken relatively close to the surface. Although not a component of the analysis here, the large variability in horizontal-leg CO_2 mole fraction near the PBL, more modest horizontal-leg variations in the FT, and the importance of characterizing the PBL depth accurately to estimate PBL CO_2 mole fraction, imply that this simple characterization of the mole-fraction gradient between the FT and PBL may be misleading.

Finally, having continuous observations allows the quantification of the error associated with the mean value for a given elevation or atmospheric layer, due to spatio-temporal variability and instrument error. Such error characterization allows quantitative error propagation in studies using these data.

4 Conclusions

The ten years of atmospheric CO_2 profiles presented here show the strong influence of land surface fluxes on PBL-FT gradients and how they vary seasonally, and the continental influence on the amplitude of seasonal variability in mole fraction. The secular increase in the FT atmospheric CO_2 mole fraction at SGP was consistent with the trend at Mauna Loa of 1.95 ppm yr^{-1}.

There was substantial variability in the CO_2 mole fraction over the 5–10 min horizontal legs, generally larger within the PBL and smaller in the FT. A better understanding of the source of this fine-scale variability would give insight into controls on vertical transport mechanisms for atmospheric CO_2 and improve atmospheric inversions.

To test whether comparability goals have been met, for example the WMO/GAW target of ≤ 0.1 ppm, we recommend that multiple technologies be deployed on each airborne platform. From our experience in the field, no single technology can be assumed to provide objective observations on a long-term basis. The combination of duplicate continuous instruments and flask collection gives rigorous diagnostics and a well-defined confidence level, and can be used to validate an objective sampling strategy when high precision and accuracy are required.

Acknowledgements. This research was supported by the Office of Biological and Environmental Research of the US Department of Energy under contract No. DE-AC02-05CH11231 as part of the Atmospheric Radiation Measurement Program (ARM), ARM Aerial Facility, and Terrestrial Ecosystem Science Program. AOS was supported by SBIR grants over a ten year period from the US Department of Commerce, the US Department of Energy and the National Aeronautics and Space Administration. The authors thank their colleagues for continuing support and discussion during the coffee breaks; The Greenwood group and pilot Bob Fristoe for their dedication to the program.

Edited by: D. Griffith

References

Abshire, J. B., Riris, H., Allan, G. R., Weaver, C. J., Mao, J. P., Sun, X., Hasselbrack, W. L., Kawa, S. R., and Biraud, S.: Pulsed airborne lidar measurements of atmospheric CO_2 column absorption, Tellus B, 62, 770–783, 2010.

Ackerman, T. P., Genio, A. D. D., Ellingson, R. G., Ferrare, R. A., Klein, S. A., McFarquhar, G. M., Lamb, P. J., Long, C. N., and Verlinde, J.: Atmospheric radiation measurement program science plan: current status and future direcitons of the ARM science program, US Department of Energy, Office of Biological and Environmental Research, Washington, DC, 2004.

Bakwin, P. S., Tans, P. P., Hurst, D. F., and Zhao, C. L.: Measurements of carbon dioxide on very tall towers: results of the NOAA/CMDL program, Tellus B, 50, 401–415, 1998.

Billesbach, D. P., Fischer, M. L., Torn, M. S., and Berry, J. A.: A portable eddy covariance system for the measurement of ecosystem-atmosphere exchange of CO_2, water vapor, and energy, J. Atmos. Ocean. Tech., 21, 639–650, 2004.

Carouge, C., Rayner, P. J., Peylin, P., Bousquet, P., Chevallier, F., and Ciais, P.: What can we learn from European continuous at-

mospheric CO_2 measurements to quantify regional fluxes – Part 2: Sensitivity of flux accuracy to inverse setup, Atmos. Chem. Phys., 10, 3119–3129, doi:10.5194/acp-10-3119-2010, 2010.

Chen, H., Winderlich, J., Gerbig, C., Hoefer, A., Rella, C. W., Crosson, E. R., Van Pelt, A. D., Steinbach, J., Kolle, O., Beck, V., Daube, B. C., Gottlieb, E. W., Chow, V. Y., Santoni, G. W., and Wofsy, S. C.: High-accuracy continuous airborne measurements of greenhouse gases (CO_2 and CH_4) using the cavity ring-down spectroscopy (CRDS) technique, Atmos. Meas. Tech., 3, 375–386, doi:10.5194/amt-3-375-2010, 2010.

Choi, Y. H., Vay, S. A., Vadrevu, K. P., Soja, A. J., Woo, J. H., Nolf, S. R., Sachse, G. W., Diskin, G. S., Blake, D. R., Blake, N. J., Singh, H. B., Avery, M. A., Fried, A., Pfister, L., and Fuelberg, H. E.: Characteristics of the atmospheric CO_2 signal as observed over the conterminous United States during INTEX-N A., J. Geophys. Res.-Atmos., 113, D07301, doi:10.1029/2007jd008899, 2008.

Ciais, P., Rayner, P., Chevallier, F., Bousquet, P., Logan, M., Peylin, P., and Ramonet, M.: Atmospheric inversions for estimating CO_2 fluxes: methods and perspectives, Climatic Change, 103, 69–92, 2010.

Conway, T. J., Tans, P. P., Waterman, L. S., and Thoning, K. W.: Evidence for interannual variability of the carbon-cycle from the national-oceanic-and-atmospheric-administration climate-monitoring-and-diagnostics-laboratory global-air-sampling-network, J. Geophys. Res.-Atmos., 99, 22831–22855, 1994.

Denning, A. S., Fung, I. Y., and Randall, D.: Latitudinal gradient of atmospheric CO_2 due to seasonal exchange with land biota, Nature, 376, 240–243, 1995.

Enting, I. G. and Mansbridge, J. V.: Latitudinal distribution of sources and sinks of CO_2 – results of an inversion study, Tellus B, 43, 156–170, 1991.

Enting, I. G., Trudinger, C. M., and Francey, R. J.: A synthesis inversion of the concentration and Delta-C-13 of atmospheric CO_2, Tellus B, 47, 35–52, 1995.

Fischer, M. L., Torn, M. S., Billesbach, D. P., Doyle, G., Northup, B., and Biraud, S. C.: Carbon, Water, and Heat Flux Responses to Experimental Burning and Drought in a Tallgrass Prairie, Agr. Forest Meteorol., 166–167, 169–174, 2012.

Font, A., Morgui, J. A., and Rodo, X.: Atmospheric CO_2 in situ measurements: Two examples of Crown Design flights in NE Spain, J. Geophys. Res.-Atmos., 113, D12308, doi:10.1029/2007JD009111, 2008.

Friedlingstein, P., Cox, P., Betts, R., Bopp, L., Von Bloh, W. W., Brovkin, V., Cadule, P., Doney, S., Eby, M., Fung, I., Bala, G., John, J., Jones, C., Joos, F., Kato, T., Kawamiya, M., Knorr, W., Lindsay, K., Matthews, H. D., Raddatz, T., Rayner, P., Reick, C., Roeckner, E., Schnitzler, K. G., Schnur, R., Strassmann, K., Weaver, A. J., Yoshikawa, C., and Zeng, N.: Climatecarbon cycle feedback analysis: results from the C4MIP model intercomparison, J. Climate, 19, 3337–3353, 2006.

Gerbig, C., Lin, J. C., Wofsy, S. C., Daube, B. C., Andrews, A. E., Stephens, B. B., Bakwin, P. S., and Grainger, C. A.: Toward constraining regional-scale fluxes of CO_2 with atmospheric observations over a continent: 1. Observed spatial variability from airborne platforms, J. Geophys. Res.-Atmos., 108, 4756, doi:10.1029/2002jd003018, 2003.

Gurney, K. R., Law, R. M., Denning, A. S., Rayner, P. J., Baker, D., Bousquet, P., Bruhwiler, L., Chen, Y. H., Ciais, P., Fan, S., Fung, I. Y., Gloor, M., Heimann, M., Higuchi, K., John, J., Maki, T., Maksyutov, S., Masarie, K., Peylin, P., Prather, M., Pak, B. C., Randerson, J., Sarmiento, J., Taguchi, S., Takahashi, T., and Yuen, C. W.: Towards robust regional estimates of CO_2 sources and sinks using atmospheric transport models, Nature, 415, 626–630, 2002.

Gurney, K. R., Law, R. M., Denning, A. S., Rayner, P. J., Pak, B. C., Baker, D., Bousquet, P., Bruhwiler, L., Chen, Y. H., Ciais, P., Fung, I. Y., Heimann, M., John, J., Maki, T., Maksyutov, S., Peylin, P., Prather, M., and Taguchi, S.: Transcom 3 inversion intercomparison: model mean results for the estimation of seasonal carbon sources and sinks, Global Biogeochem. Cy., 18, GB1010, doi:10.1029/2003GB002111, 2004.

Haszpra, L., Ramonet, M., Schmidt, M., Barcza, Z., Pátkai, Zs., Tarczay, K., Yver, C., Tarniewicz, J., and Ciais, P.: Variation of CO_2 mole fraction in the lower free troposphere, in the boundary layer and at the surface, Atmos. Chem. Phys., 12, 8865–8875, doi:10.5194/acp-12-8865-2012, 2012.

Helliker, B. R., Berry, J. A., Betts, A. K., Bakwin, P. S., Davis, K. J., Denning, A. S., Ehleringer, J. R., Miller, J. B., Butler, M. P., and Ricciuto, D. M.: Estimates of net CO_2 flux by application of equilibrium boundary layer concepts to CO_2 and water vapor measurements from a tall tower, J. Geophys. Res.-Atmos., 109, D20106, doi:10.1029/2004jd004532, 2004.

Hill, T. C., Williams, M., Woodward, F. I., and Moncrieff, J. B.: Constraining ecosystem processes from tower fluxes and atmospheric profiles, Ecol. Appl., 21, 1474–1489, 2011.

Huntzinger, D. N., Gourdji, S. M., Mueller, K. L., and Michalak, A. M.: A systematic approach for comparing modeled biospheric carbon fluxes across regional scales, Biogeosciences, 8, 1579–1593, doi:10.5194/bg-8-1579-2011, 2011.

IPCC: Climate Change 2007: The Physical Science Basis. Contribution of Working Group I to the Fourth Assessment Report of the IPCC, Cambridge University Press, Cambridge, UK and New York, 2007.

Karion, A., Sweeney, C., Wolter, S., Newberger, T., Chen, H., Andrews, A., Kofler, J., Neff, D., and Tans, P.: Long-term greenhouse gas measurements from aircraft, Atmos. Meas. Tech., 6, 511–526, doi:10.5194/amt-6-511-2013, 2013.

Keeling, C. D.: The concentration and isotopic abundances of carbon dioxide in the atmosphere, Tellus, 12, 200–203, 1960.

Kuai, L., Worden, J., Kulawik, S., Bowman, K., Lee, M., Biraud, S. C., Abshire, J. B., Wofsy, S. C., Natraj, V., Frankenberg, C., Wunch, D., Connor, B., Miller, C., Roehl, C., Shia, R.-L., and Yung, Y.: Profiling tropospheric CO_2 using Aura TES and TCCON instruments, Atmos. Meas. Tech., 6, 63–79, doi:10.5194/amt-6-63-2013, 2013.

Kulawik, S. S., Jones, D. B. A., Nassar, R., Irion, F. W., Worden, J. R., Bowman, K. W., Machida, T., Matsueda, H., Sawa, Y., Biraud, S. C., Fischer, M. L., and Jacobson, A. R.: Characterization of Tropospheric Emission Spectrometer (TES) CO2 for carbon cycle science, Atmos. Chem. Phys., 10, 5601-5623, doi:10.5194/acp-10-5601-2010, 2010.

Kulawik, S. S., Worden, J. R., Wofsy, S. C., Biraud, S. C., Nassar, R., Jones, D. B. A., Olsen, E. T., and Osterman, and the TES and HIPPO teams, G. B.: Comparison of improved Aura Tropospheric Emission Spectrometer (TES) CO_2 with HIPPO and SGP

aircraft profile measurements, Atmos. Chem. Phys. Discuss., 12, 6283–6329, doi:10.5194/acpd-12-6283-2012, 2012.

Langenfelds, R. L., Francey, R. J., Steele, L. P., Dunse, B. L., Butler, T. M., Spencer, D. A., Kivlighon, L. M., and Meyer, C. P.: Flask sampling from Cape Grim overflights. Baseline Atmospheric Program (Australia) 1999–2000, edited by: Tindale, N. W., Derek, N., and Fraser, P. J., Bureau of Meteorology and CSIRO Atmospheric Research, Melbourne, Australia, 73–75, 2003.

Lin, J. C., Gerbig, C., Wofsy, S. C., Andrews, A. E., Daube, B. C., Grainger, C. A., Stephens, B. B., Bakwin, P. S., and Hollinger, D. Y.: Measuring fluxes of trace gases at regional scales by Lagrangian observations: application to the CO_2 budget and rectification airborne (COBRA) study, J. Geophys. Res.-Atmos., 109, D15304, doi:10.1029/2004JD004754, 2004.

Marquis, M. and Tans, P.: Climate change – carbon crucible, Science, 320, 460–461, 2008.

Masarie, K. A., Langenfelds, R. L., Allison, C. E., Conway, T. J., Dlugokencky, E. J., Francey, R. J., Novelli, P. C., Steele, L. P., Tans, P. P., Vaughn, B., and White, J. W. C.: NOAA/CSIRO flask air intercomparison experiment: a strategy for directly assessing consistency among atmospheric measurements made by independent laboratories, J. Geophys. Res.-Atmos., 106, 20445–20464, 2001.

Mays, K. L., Shepson, P. B., Stirm, B. H., Karion, A., Sweeney, C., and Gurney, K. R.: Aircraft based measurements of the carbon footprint of Indianapolis, Environ. Sci. Technol., 43, 7816–7823, 2009.

NACP SIS: available at: http://www.nacarbon.org/nacp/documents/NACP-SIS-final-july05.pdf (last access: 24 September 2012), 2005.

Pales, J. C. and Keeling, C. D.: Concentration of atmospheric carbon dioxide in Hawaii, J. Geophys. Res., 70, 6053–6076, 1965.

Pataki, D. E., Xu, T., Luo, Y. Q., and Ehleringer, J. R.: Inferring biogenic and anthropogenic carbon dioxide sources across an urban to rural gradient, Oecologia, 152, 307–322, 2007.

Pearman, G. I., Hyson, P., and Fraser, P. J.: The global distribution of atmospheric carbondioxide. 1: Aspects of observations and modeling, J. Geophys. Res.-Ocean Atmos., 88, 3581–3590, 1983.

Peters, W., Jacobson, A. R., Sweeney, C., Andrews, A. E., Conway, T. J., Hughes, J., Schaefer, K., Masarie, K. A., Jacobson, A. R., Miller, J. B., Cho, C. H., Ramonet, M., Schmidt, M., Ciattaglia, L., Apadula, F., Helta, D., Meinhardt, F., di Sarra, A. G., Piacentino, S., Sferlazzo, D., Aalto, T., Hatakka, J., Strom, J., Haszpra, L., Meijer, H. A. J., van der Laan, S., Neubert, R. E. M., Jordan, A., Rodo, X., Morgui, J. A., Vermeulen, A. T., Popa, E., Rozanski, K., Zimnoch, M., Manning, A. C., Leuenberger, M., Uglietti, C., Dolman, A. J., Ciais, P., Heimann, M., and Tans, P. P.: An atmospheric perspective on North American carbon dioxide exchange: carbontracker, P. Natl. Acad. Sci. USA, 104, 18925–18930, 2007.

Peters, W., Krol, M. C., van der Werf, G. R., Houweling, S., Jones, C. D., Bousquet, P., Peylin, P., Maksyutov, S., Marshall, J., Rodenbeck, C., Langenfelds, R. L., Steele, L. P., Francey, R. J., Tans, P., and Sweeney, C.: Seven years of recent European net terrestrial carbon dioxide exchange constrained by atmospheric observations, Global. Change. Biol., 16, 1317–1337, 2010.

Pickett-Heaps, C. A., Rayner, P. J., Law, R. M., Ciais, P., Patra, P. K., Bousquet, P., Peylin, P., Maksyutov, S., Marshall, J., Rödenbeck, C., Langenfelds, R. L., Steele, L. P., Francey, R. J., Tans, P., and Sweeney, C.: Atmospheric CO_2 inversion validation using vertical profile measurements: analysis of four independent inversion models, J. Geophys. Res.-Atmos, 116, D12305, doi:10.1029/2010jd014887, 2011.

Rayner, P. J., Enting, I. G., Francey, R. J., and Langenfelds, R.: Reconstructing the recent carbon cycle from atmospheric CO_2, delta C-13 and O_2/N_2 observations, Tellus B, 51, 213–232, 1999.

Rayner, P. J., Law, R. M., O'Brien, D. M., Butler, T. M., and Dilley, A. C.: Global observations of the carbon budget – 3. Initial assessment of the impact of satellite orbit, scan geometry, and cloud on measuring CO_2 from space, J. Geophys. Res.-Atmos, 107, 4557, doi:10.1029/2001JD000618, 2002.

Riley, W. J., Biraud, S. C., Torn, M. S., Fischer, M. L., Billesbach, D. P., and Berry, J. A.: Regional CO_2 and latent heat surface fluxes in the Southern Great Plains: measurements, modeling, and scaling, J. Geophys. Res.-Biogeo., 114, G04009, doi:10.1029/2009JG001003, 2009.

Shepson, P. B., Cambaliza, M., Davis, K., Gurney, K., Lauvaux, T., Richardson, N., Richardson, S., Sweeney, C., and Turnbull, J.: Indianapolis flux experiment (INFLUX): experiment design and new results regarding measurements of urban-area CO_2 and CH_4 emission fluxes, Abstr. Pap. Am. Chem. S., Vol. 242, 2011.

Stephens, B. B., Gurney, K. R., Tans, P. P., Sweeney, C., Peters, W., Bruhwiler, L., Ciais, P., Ramonet, M., Bousquet, P., Nakazawa, T., Aoki, S., Machida, T., Inoue, G., Vinnichenko, N., Lloyd, J., Jordan, A., Heimann, M., Shibistova, O., Langenfelds, R. L., Steele, L. P., Francey, R. J., and Denning, A. S.: Weak northern and strong tropical land carbon uptake from vertical profiles of atmospheric CO_2, Science, 316, 1732–1735, 2007.

Stephens, B. B., Miles, N. L., Richardson, S. J., Watt, A. S., and Davis, K. J.: Atmospheric CO_2 monitoring with single-cell NDIR-based analyzers, Atmos. Meas. Tech., 4, 2737–2748, doi:10.5194/amt-4-2737-2011, 2011.

Stull, R. B.: An Introduction to Boundary Layer Meteorology, Kluwer Academic, Boston, Mass, 666 pp., 1988.

Tans, P. P., Thoning, K. W., Elliott, W. P., and Conway, T. J.: Error-estimates of background atmospheric CO_2 patterns from weekly flask samples, J. Geophys. Res.-Atmos, 95, 14063–14070, 1990.

Williams, I. N., Riley, W. J., Torn, M. S., Berry, J. A., and Biraud, S. C.: Using boundary layer equilibrium to reduce uncertainties in transport models and CO_2 flux inversions, Atmos. Chem. Phys., 11, 9631–9641, doi:10.5194/acp-11-9631-2011, 2011.

WMO: Report of the 15th WMO/IAEA meeting of experts on carbon dioxide, other greenhouse gases, and related tracers measurement techniques, Jena, Germany, 2011.

Wunch, D., Toon, G. C., Wennberg, P. O., Wofsy, S. C., Stephens, B. B., Fischer, M. L., Uchino, O., Abshire, J. B., Bernath, P., Biraud, S. C., Blavier, J.-F. L., Boone, C., Bowman, K. P., Browell, E. V., Campos, T., Connor, B. J., Daube, B. C., Deutscher, N. M., Diao, M., Elkins, J. W., Gerbig, C., Gottlieb, E., Griffith, D. W. T., Hurst, D. F., Jiménez, R., Keppel-Aleks, G., Kort, E. A., Macatangay, R., Machida, T., Matsueda, H., Moore, F., Morino, I., Park, S., Robinson, J., Roehl, C. M., Sawa, Y., Sherlock, V., Sweeney, C., Tanaka, T., and Zondlo, M. A.: Calibration of the Total Carbon Column Observing Network using aircraft profile data, Atmos. Meas. Tech., 3, 1351–1362, doi:10.5194/amt-

3-1351-2010, 2010.

Wunch, D., Wennberg, P. O., Toon, G. C., Connor, B. J., Fisher, B., Osterman, G. B., Frankenberg, C., Mandrake, L., O'Dell, C., Ahonen, P., Biraud, S. C., Castano, R., Cressie, N., Crisp, D., Deutscher, N. M., Eldering, A., Fisher, M. L., Griffith, D. W. T., Gunson, M., Heikkinen, P., Keppel-Aleks, G., Kyrö, E., Lindenmaier, R., Macatangay, R., Mendonca, J., Messerschmidt, J., Miller, C. E., Morino, I., Notholt, J., Oyafuso, F. A., Rettinger, M., Robinson, J., Roehl, C. M., Salawitch, R. J., Sherlock, V., Strong, K., Sussmann, R., Tanaka, T., Thompson, D. R., Uchino, O., Warneke, T., and Wofsy, S. C.: A method for evaluating bias in global measurements of CO_2 total columns from space, Atmos. Chem. Phys., 11, 12317–12337, doi:10.5194/acp-11-12317-2011, 2011.

Xueref-Remy, I., Messager, C., Filippi, D., Pastel, M., Nedelec, P., Ramonet, M., Paris, J. D., and Ciais, P.: Variability and budget of CO_2 in Europe: analysis of the CAATER airborne campaigns – Part 1: Observed variability, Atmos. Chem. Phys., 11, 5655–5672, doi:10.5194/acp-11-5655-2011, 2011.